D. S. Dolitskavich

FED-Vol. 164

ELECTRO-RHEOLOGICAL FLOWS – 1993

presented at
THE FLUIDS ENGINEERING CONFERENCE
WASHINGTON, D.C.
JUNE 20-24, 1993

sponsored by
THE FLUIDS ENGINEERING DIVISION, ASME

edited by
D. A. SIGINER
AUBURN UNIVERSITY

J. H. KIM
ELECTRIC POWER RESEARCH INSTITUTE

R. A. BAJURA
WEST VIRGINIA UNIVERSITY

THE
AMERICAN SOCIETY
OF MECHANICAL ENGINEERS
UNITED ENGINEERING CENTER
345 East 47th Street New York, N.Y. 10017

FED-Vol. 164, Electro-Rheological Flows
ASME 1993

COMPUTATIONS OF ELECTRO-THERMO-CONVECTIVE PHENOMENA IN ELECTRO-RHEOLOGICAL FLUIDS

Seungsoo Lee
Agency for Defense Development
Taejon, Korea

George S. Dulikravich and Vineet Ahuja
Department of Aerospace Engineering
Pennsylvania State University
University Park, Pennsylvania

Abstract

A complete system of partial differential equations governing three-dimensional laminar flow of an incompressible viscous neutrally charged carrier fluid injected with an electrically charged fluid has been elaborated. The model accounts for temperature dependent physical properties via an extended Boussinesq approximation while including a Joule heating effect. The system of coupled partial differential equations was solved using an artificial compressibility formulation and explicit finite differencing with a four-step Runge-Kutta time integration. Two-dimensional numerical results demonstrate cases of electrohydrodynamic instability in horizontal and vertical closed containers. Simulations of the plane Couette flow under the influence of a steady electric field is also demonstrated including the results where viscosity was treated as a function of local electric charge concentrations.

Nomenclature:

$\tilde{\mathbf{A}}$ = ξ-flux vector Jacobian in curvilinear coordinates
AR = aspect ratio of a container (length/height)
b = charged particles mobility coefficient [$m^2\ s^{-1}\ V^{-1}$]
$\tilde{\mathbf{B}}$ = η-flux vector Jacobian in curvilinear coordinates
c = specific heat coefficient [$m^2\ K^{-1}\ s^{-2}$]
$\tilde{\mathbf{C}}$ = ζ-flux vector Jacobian in curvilinear coordinates
D = diffusivity coefficient of charged particles [$m^2\ s^{-1}$]
D = differential operator
$\mathbf{D}$ = diagonal matrix
$E\ (E_x, E_y, E_z)^T$ = electric field vector [$V\ m^{-1}$]
$\mathbf{E}$ = x-flux vector in Cartesian coordinates
$\tilde{\mathbf{E}}$ = ξ-flux vector in curvilinear coordinates
$\mathbf{F}$ = y-flux vector in Cartesian coordinates
$\tilde{\mathbf{F}}$ = η-flux vector in curvilinear coordinates
g_{ij} = metric tensor
$\mathbf{g}(g_x, g_y, g_z)^T$ = gravity acceleration vector [$m\ s^{-2}$]
$\mathbf{G}$ = z-flux vector in Cartesian coordinates
$\tilde{\mathbf{G}}$ = ζ-flux vector in curvilinear coordinates
$\mathbf{J}$ = electric current per unit volume [$A\ m^{-3}$]

$\mathbf{I}$ = identity matrix
k = heat conductivity coefficient [kg m s^{-3} K^{-1}]
k_B = Boltzman's constant [kg^{-1} s K]
l = length [m]
$\mathbf{L}$ = selection matrix
$\mathbf{M}$ = modal matrix
$\mathbf{n}$ = unit vector normal to the solid wall
p = fluid pressure [N m^{-2}]
q = electric charge density per unit volume [kg m^{-1} s^{-2} V^{-1}]
$\tilde{\mathbf{R}}$ = residual vector
$\mathbf{Q}$ = solution vector in Cartesian coordinates
$\tilde{\mathbf{Q}}$ = solution vector in curvilinear coordinates
$\tilde{\mathbf{R}}$ = residual vector
$\mathbf{S}$ = source term vector in Cartesian coordinates
$\tilde{\mathbf{S}}$ = source term vector in curvilinear coordinates
t = time [s]
T = temperature [K]
ΔT = temperature difference [K]
U, V, W = contravariant velocity components [m s^{-1}]
v(u,v,w) = velocity vector in Cartesian coordinates [m s^{-1}]
x,y,z = Cartesian coordinates [m]
α = thermal expansion coefficient [K^{-1}]
β = artificial compressibility coefficient
δ = smoothing operator
ε = electrical permitivity coefficient [kg m s^{-2} V^{-2}]
ε_2 = second order artificial dissipation parameter
ε_4 = fourth order artificial dissipation parameter
ϕ = gravity potential [m^{-2} s^{-2}]
φ = electric potential [V]
$\tilde{\lambda}$ = eigenmatrix of a Jacobian flux vector
ξ,η,ζ= curvilinear coordinates [m]
η = viscosity coefficient [kg m^{-1} s^{-1}]
ω = smoothing coefficient for residual
Ω = boundary condition vector
ψ = artificial dissipation sensor function
ρ = fluid density [kg m^{-3}]
θ = nondimensional temperature difference

subscripts
c = cold wall
E = electrical
h = hot wall
o = reference values

superscripts
* = nondimensional values
T = transpose of a matrix

1. INTRODUCTION

Two extreme models for a fluid flow under the influence of electromagnetic fields have been derived in the fundamental paper by Stuetzer (1962). The models are Magnetohydrodynamics (MHD) and Electrohydrodynamics (EHD). The MHD model assumes that there are no charged particles in the

flow field and that there is no electric potential applied or induced. These types of flows have been discussed in a number of publications (Lee and Dulikravich, 1991a; Dulikravich and Kosovic, 1992; Dulikravich, Ahuja and Lee, 1993). EHD model on the other hand assumes that there is no magnetic field applied or induced (Stuetzer, 1962; Landau and Lifshitz, 1960; Melcher, 1981; Babskii et al, 1989; Eringen and Maugin, 1990a and 1990b; Reitz et al., 1979). Instead, an external electric field is applied to an electrically conducting fluid containing electrically charged particles. These particles are convected with the flow field in the case when there is a mean flow. At the same time, the charged particles can diffuse and move (Reitz et al., 1979; Rhodes and Snyder, 1989; Changeart et al, 1986; Bello and Polezhaev, 1991; Lee, Dulikravich and Kosovic, 1991) under the influence of the outside (imposed) and inside (self-induced) electric field. When modeling EHD flows, in addition to complete Navier-Stokes equations, one should add an equation for electric charge preservation for each of the electrically charged species (Babskii et al, 1989). One equation governing the electric potential field must also be added. In the momentum equation we will include a thermal buoyancy force using the extended Boussinesq approximation (Gray and Giorgini, 1976) and an electrical (Lorentz) body force (Stuetzer, 1962; Lee, Dulikravich and Kosovic, 1991). In the energy equation we will add a Joule heating term (Lee, Dulikravich and Kosovic, 1991), while neglecting viscous dissipation in accordance with the Boussinesq approximation. Although relatively well documented analytical models for EHD flows have been developed, somewhat incomplete versions of these models have been numerically solved (Changeart et al, 1986; Bello and Polezhaev, 1991; Lee, Dulikravich and Kosovic, 1991) in the past. The objective of this paper is to present a fully three-dimensional mathematical model, a numerical algorithm for its solution and computational results for cases of two-dimensional steady laminar EHD flows in closed containers and in channels. The present model accounts for a single specie of charged fluid. This model can be easily extended to multi-species formulation (Babskii et al, 1989) including non-neutral carrier fluids.

2. ANALYTICAL MODEL

The system of governing equations (Stuetzer, 1962; Lee, Dulikravich and Kosovic, 1991) can be derived from a combination of Maxwell's equations of electrodynamics and the Navier-Stokes equations. Maxwell's equations in International System of units (Reitz et al, 1979) using tensor notation, are

$$D_{i,t} = \varepsilon_{ijk} H_{k,j} - J_i \tag{1}$$

$$B_{i,t} = - \varepsilon_{ijk} E_{k,j} \tag{2}$$

$$D_{i,i} = q \tag{3}$$

$$B_{i,i} = 0 \tag{4}$$

where J_i, H_k, E_k, q are the electric current density, magnetic field vector, electric field vector, and electric charge density, respectively. A comma denotes differentiation. The electric displacement vector D_i and magnetic displacement vector B_i are defined as

$$D_i = \varepsilon E_i + P_i \tag{5}$$

$$B_i = \mu H_i + M_i \tag{6}$$

where P_i is the electric polarization displacement, M_i is the magnetization vector, ε is the dielectric constant, and μ is the magnetic permeability. An idealized charged fluid is assumed in this electrohydrodynamic model (Stuetzer, 1962) and therefore magnetic fields can be neglected. The magnetic field vector B_i and the electric polarization vector P_i are small compared to E_i and thus can be neglected. Finally, Maxwell's equations are reduced to

$$\varepsilon E_{i,t} = - J_i \tag{7}$$

$$\varepsilon_{ijk} E_{k,j} = 0 \tag{8}$$

$$\varepsilon E_i = q \tag{9}$$

where it was assumed that electric constant, ε is constant. Finally, introducing equation (9) in equation (7), Maxwell's equations reduce to charge conservation equation and Poisson's partial differential equation for electric potential since the electric field E_i is irrotational. The incompressible form of the Navier-Stokes equations has been modified in order to take into account the effects of thermal buoyancy force, Lorentz force and Joule heating. In accordance with the extended Boussinesq approximation (Gray and Giorgini, 1976; Lee, Dulikravich and Kosovic, 1991) , density of the fluid was assumed to be a function of temperature. Buoyancy force and Lorentz force are body forces and they were introduced into the system as source terms in the momentum conservation equation, while Joule heating term represents a source term in the energy conservation equation. Thus the governing equations are

Continuity

$$\nabla \cdot \mathbf{v} = 0 \tag{10}$$

Momentum (including thermal buoyancy force and electric Lorentz force)

$$\rho_o \frac{D\mathbf{v}}{Dt} = -\nabla p - \rho_o \alpha \mathbf{g} \Delta T + \nabla \cdot (\eta_o \nabla \mathbf{v}) + q \boldsymbol{E} \tag{11}$$

Energy (including Joule heating)

$$\rho c \frac{DT}{Dt} = \nabla \cdot (k \nabla T) + \mathbf{J} \cdot \boldsymbol{E} \tag{12}$$

Electric charge conservation

$$\frac{\partial q}{\partial t} + \nabla \cdot \mathbf{J} = 0 \tag{13}$$

Electric potential field

$$\nabla \cdot \boldsymbol{E} = \frac{q}{\varepsilon} \tag{14}$$

The induced electric current per unit volume is given by Ohm's law

$$\mathbf{J} = q (\mathbf{v} + b \boldsymbol{E}) - D \nabla q \tag{15}$$

The electric charge diffusivity coefficient D and mobility coefficient b are related by Einstein's formula (Babski et al, 1989)

$$D = \frac{k_B T}{q m_i} \rho_i b \tag{16}$$

where m_i is the mass of a charged particle and ρ_i is the density of the electrically non-neutral fluid. Since the electric field is irrotational, it follows that

$$\nabla \times \boldsymbol{E} = 0 \tag{17}$$

$$\boldsymbol{E} = -\nabla \varphi \tag{18}$$

where φ is the electric potential, so that equation (14) becomes

$$\nabla^2 \varphi = -\frac{q}{\varepsilon} \tag{19}$$

Nondimensionalization can be performed with respect to the reference values denoted by subscript o, so that

$$\mathbf{v}^* = \frac{\mathbf{v}}{v_o} \qquad \mathbf{x}^* = \frac{\mathbf{x}}{x_o} \qquad t^* = \frac{t\, v_o}{l_o} \qquad p^* = \frac{p}{\rho_o\, v_o^2} \tag{20}$$

$$\varphi^* = \frac{\Delta\varphi}{\Delta\varphi_o} \qquad \boldsymbol{E}^* = \frac{\boldsymbol{E}\, l_o}{\Delta\varphi_o} \qquad q^* = \frac{q}{q_o} \qquad \theta = \frac{\Delta T}{\Delta T_o} \qquad g^* = \frac{g}{g_o} \tag{21}$$

If T_c is the temperature of the cold wall and T_h is the temperature of the hot wall, then $\Delta T = T - T_c$ and $\Delta T_o = T_h - T_c$. Similarly, $\Delta\varphi_o$ is the reference value of the difference of the electric potential between the two electrodes. Fluid density, electric charge mobility and coefficients of specific heat, thermal expansion, viscosity and heat conduction can be expressed (Gray and Giorgini, 1976; Lee, Dulikravich and Kosovic, 1991) as

$$\rho = \rho_o\, \rho'(\theta) \qquad b = b_o\, b'(\theta) \qquad c = c_o\, c'(\theta) \tag{22}$$

$$\alpha = \alpha_o\, \alpha'(\theta) \qquad \eta = \eta_o\, \eta'(\theta) \qquad k = k_o\, k'(\theta) \tag{23}$$

where the primed values denote arbitrary functions of non-dimensional temperature, θ. The following nondimensional groups should be introduced as

Reynolds number	$\mathrm{Re} = \dfrac{\rho_o\, v_o\, l_o}{\eta_o}$	Lorentz force number	$S_E = \dfrac{q_o\, \Delta\varphi_o}{\rho_o\, v_o^2}$
Prandtl number	$\mathrm{Pr} = \dfrac{c_o\, \eta_o}{k_o}$	Charge diffusivity number	$D_E = \dfrac{\eta_o}{\rho_o\, D_o}$
Grashof number	$\mathrm{Gr} = \dfrac{\rho_o^2\, g_o\, \alpha_o\, \Delta T_o\, l_o^3}{\eta_o^2}$	Electric Prandtl number	$\mathrm{Pr}_E = \dfrac{\eta_o}{\rho_o\, b_o\, \Delta\varphi_o}$
Eckert number	$\mathrm{Ec} = \dfrac{v_o^2}{c_o\, \Delta T_o}$	Electric field number	$N_E = \dfrac{q_o\, l_o^2}{\varepsilon_o\, \Delta\varphi_o}$
Froude number	$\mathrm{Fr}^2 = \dfrac{v_o^2}{g_o\, l_o}$		

(24)

The non-dimensional density ρ' can be expanded in a Taylor series while retaining only the first order term

$$\rho' = 1 - \alpha\, \Delta T = 1 - \alpha^*\, \theta \tag{25}$$

where

$$\alpha^* = \frac{\partial \rho'}{\partial \theta} = \frac{\partial \rho'}{\partial \theta}\frac{\Delta T_o\, \rho_o}{\rho_o\, \Delta T_o} = \frac{1}{\rho_o}\frac{\partial \rho}{\partial T}\Delta T_o = \alpha\, \Delta T_o \tag{26}$$

It can be assumed that the coefficient of thermal expansion, α, is constant in the range of temperatures

which are of interest in a particular case. When the term $(\alpha \Delta T_o) \ll 1$, starting with the complete Navier-Stokes equations for compressible fluid flow, equations more general than what is known as the Boussinesq approximation can be derived (Gray and Giorgini, 1976; Lee, Dulikravich and Kosovic, 1991) for the fluid with non-constant properties. Thus, the system of equations (10-19) for incompressible flow of a fluid with temperature dependent properties and electric charges under the influence of an electric field can be reduced (Lee, Dulikravich and Kosovic, 1991) to

$$\nabla^* \cdot \mathbf{v}^* = 0 \tag{27}$$

$$\frac{\partial \mathbf{v}^*}{\partial t^*} + \nabla^* \cdot (\mathbf{v}^* \mathbf{v}^* + \bar{\bar{p}}^* \mathbf{1}) = \frac{1}{Re} \nabla^* \cdot (\eta' \nabla^* \mathbf{v}^*) + \frac{Gr\, \theta}{Re^2} \mathbf{g}^* + S_E q^* \boldsymbol{E}^* \tag{28}$$

$$\frac{\partial \theta}{\partial t^*} + \nabla^* \cdot (\theta^* \mathbf{v}^*) = \frac{1}{Pr\, Re\, c'} \nabla^* \cdot (k' \nabla^* \theta)$$

$$+ \frac{S_E\, Ec}{c'} \left(q^* \left(\mathbf{v}^* + \frac{1}{Re\, Pr_E} \boldsymbol{E}^* \right) - \frac{1}{Re\, D_E} \nabla^* q^* \right) \cdot \boldsymbol{E}^* \tag{29}$$

$$\frac{\partial q^*}{\partial t^*} + \nabla^* \cdot \left(q^* \left(\mathbf{v}^* + \frac{1}{Re\, Pr_E} \boldsymbol{E}^* \right) \right) = \frac{1}{Re} \nabla^* \cdot \left(\frac{1}{D_E} b' \nabla^* q^* \right) \tag{30}$$

$$\nabla^{*2} \varphi^* = - N_E q^* \tag{31}$$

where $\bar{\bar{p}}^* = p^* + \frac{\phi^*}{Fr^2}$ so that $\mathbf{g}^* = \nabla^* \phi^*$. It should be pointed out that viscous dissipation is negligible (Gray and Giorgini, 1976; Lee, Dulikravich and Kosovic, 1991) since its ratio with respect to the convective term in the energy equation is of the order $\frac{Ec}{Re}$ which is typically a very small number.

3. NUMERICAL MODEL

Based on the mathematical model derived above, a numerical model has been developed. For simplicity and clarity of notation, the asterisk symbol in the system of equations (27-31) will be omitted. The system can be written in fully conservative vector form in physical Cartesian coordinates as follows

$$\frac{\partial \mathbf{Q}}{\partial t} + \frac{\partial \mathbf{E}}{\partial x} + \frac{\partial \mathbf{F}}{\partial y} + \frac{\partial \mathbf{G}}{\partial z} = \frac{\partial}{\partial x}\left(\mathbf{D} \frac{\partial \mathbf{Q}}{\partial x} \right) + \frac{\partial}{\partial y}\left(\mathbf{D} \frac{\partial \mathbf{Q}}{\partial y} \right) + \frac{\partial}{\partial z}\left(\mathbf{D} \frac{\partial \mathbf{Q}}{\partial z} \right) + \mathbf{S} \tag{32}$$

where the solution vector **Q** and the generalized flux vectors **E**, **F**, **G** are defined as

$$\mathbf{Q} = \begin{Bmatrix} \bar{\bar{p}}/\beta \\ u \\ v \\ w \\ \theta \\ q \end{Bmatrix} \quad \mathbf{E} = \begin{Bmatrix} u \\ u^2 + \bar{\bar{p}} \\ uv \\ uw \\ u\theta \\ q\left(u + \frac{1}{RePr_E} E_x\right) \end{Bmatrix} \quad \mathbf{F} = \begin{Bmatrix} v \\ vu \\ v^2 + \bar{\bar{p}} \\ vw \\ v\theta \\ q\left(v + \frac{1}{RePr_E} E_y\right) \end{Bmatrix} \quad \mathbf{G} = \begin{Bmatrix} w \\ wu \\ wv \\ w^2 + \bar{\bar{p}} \\ w\theta \\ q\left(w + \frac{1}{RePr_E} E_z\right) \end{Bmatrix} \tag{33}$$

Here, $\frac{\partial(\bar{\bar{p}}/\beta)}{\partial t}$ represents artificial compressibility (Chorin, 1967) term which was added so that the

entire system can be made non-singular and consequently integrated simultaneously. Parameter β is a user specified value that depends on discretization quality (Lee and Dulikravich, 1991b). The source term vector **S** and diagonal matrix **D** are

$$\mathbf{S}=\begin{Bmatrix} 0 \\ \frac{Gr}{Re^2}\theta\, g_x + S_E\, q\, E_x \\ \frac{Gr}{Re^2}\theta\, g_y + S_E\, q\, E_y \\ \frac{Gr}{Re^2}\theta\, g_z + S_E\, q\, E_z \\ \frac{S_E\, Ec}{c'}\left[q\left(v+\frac{1}{RePr_E}\boldsymbol{E}\right) - \frac{1}{Re\, D_E}\nabla q\right]\cdot \boldsymbol{E} \\ 0 \end{Bmatrix} \qquad \mathbf{D}=\frac{1}{Re}\begin{Bmatrix} 0 \\ \eta' \\ \eta' \\ \eta' \\ \frac{k'}{Pr\, c'} \\ \frac{b'}{D_E} \end{Bmatrix}^T \tag{34}$$

The electric potential field equation (31) is solved separately during each iteration. After transformation to generalized curvilinear non-orthogonal coordinates in computational space, the system of governing equations can be written as

$$\frac{\partial \tilde{\mathbf{Q}}}{\partial t}+\frac{\partial \tilde{\mathbf{E}}}{\partial \xi}+\frac{\partial \tilde{\mathbf{F}}}{\partial \eta}+\frac{\partial \tilde{\mathbf{G}}}{\partial \zeta}=\frac{\partial}{\partial \xi}\left(\frac{\tilde{\mathbf{D}}}{J}\, g_{ij}\, \frac{\partial J\tilde{\mathbf{Q}}}{\partial \xi}\right)+\frac{\partial}{\partial \eta}\left(\frac{\tilde{\mathbf{D}}}{J}\, g_{ij}\, \frac{\partial J\tilde{\mathbf{Q}}}{\partial \eta}\right)+\frac{\partial}{\partial \zeta}\left(\frac{\tilde{\mathbf{D}}}{J}\, g_{ij}\, \frac{\partial J\tilde{\mathbf{Q}}}{\partial \zeta}\right)+\tilde{\mathbf{S}} \tag{35}$$

The transformed solution vector, flux and source term vectors in curvilinear coordinates are

$$\tilde{\mathbf{Q}}=\frac{1}{J}\begin{Bmatrix} \bar{\bar{p}}/\beta \\ u \\ v \\ w \\ \theta \\ q \end{Bmatrix} \quad \tilde{\mathbf{E}}=\frac{1}{J}\begin{Bmatrix} U \\ Uu + \xi_x\, \bar{\bar{p}} \\ Uv \\ Uw \\ U\theta \\ q\left(U+\frac{1}{RePr_E}E_\xi\right) \end{Bmatrix} \quad \tilde{\mathbf{F}}=\frac{1}{J}\begin{Bmatrix} V \\ Vu \\ Vv + \eta_y\, \bar{\bar{p}} \\ Vw \\ V\theta \\ q\left(V+\frac{1}{RePr_E}E_\eta\right) \end{Bmatrix} \quad \tilde{\mathbf{G}}=\frac{1}{J}\begin{Bmatrix} W \\ Wu \\ Wv \\ Ww+\zeta_z\, \bar{\bar{p}} \\ W\theta \\ q\left(W+\frac{1}{RePr_E}E_\zeta\right) \end{Bmatrix} \tag{36}$$

$$\tilde{\mathbf{S}}=\begin{Bmatrix} 0 \\ \frac{Gr}{Re^2}\theta\, g_x + S_E\, q\, E_x \\ \frac{Gr}{Re^2}\theta\, g_y + S_E\, q\, E_y \\ \frac{Gr}{Re^2}\theta\, g_z + S_E\, q\, E_z \\ \frac{S_E\, Ec}{c'}\left[q\left(v+\frac{1}{RePr_E}\boldsymbol{E}\right) - \frac{1}{Re\, D_E}\nabla q\right]\cdot \boldsymbol{E} \\ 0 \end{Bmatrix} \tag{37}$$

where $\tilde{\mathbf{D}} = \mathbf{D}$ and $J = \partial(\xi,\eta,\zeta)/\partial(x,y,z)$ is the determinant of the Jacobian geometric transformation matrix from physical x,y,z into computational ξ,η,ζ space, and g_{ij} is the metric tensor given by

$$g_{ij} = \nabla x_i' \cdot \nabla x_j' \tag{38}$$

Contravariant velocity components are related to velocity components in Cartesian coordinate system as follows

$$\begin{Bmatrix} U \\ V \\ W \end{Bmatrix} = \begin{bmatrix} \xi_{,x} & \xi_{,y} & \xi_{,z} \\ \eta_{,x} & \eta_{,y} & \eta_{,z} \\ \zeta_{,x} & \zeta_{,y} & \zeta_{,z} \end{bmatrix} \begin{Bmatrix} u \\ v \\ w \end{Bmatrix} \qquad \begin{Bmatrix} E_\xi \\ E_\eta \\ E_\zeta \end{Bmatrix} = \begin{bmatrix} \xi_{,x} & \xi_{,y} & \xi_{,z} \\ \eta_{,x} & \eta_{,y} & \eta_{,z} \\ \zeta_{,x} & \zeta_{,y} & \zeta_{,z} \end{bmatrix} \begin{Bmatrix} E_x \\ E_y \\ E_z \end{Bmatrix} \tag{39}$$

Equation (35) constitutes a system of coupled nonlinear partial differential equations. This system can be solved using a four-stage Runge-Kutta explicit time stepping method (Jameson, Schmidt and Turkel, 1981) given by

$$\begin{aligned} &\tilde{Q}^0 = \tilde{Q}^n \\ &\Delta \tilde{Q}^m = -\gamma_m \Delta t \; \tilde{R}^{m-1} \qquad\qquad m = 1,2,3,4 \\ &\tilde{Q}^{n+1} = \tilde{Q}^n + \Delta \tilde{Q}^4 \end{aligned} \tag{40}$$

The iteration level is denoted by n, and each stage of the Runge-Kutta method by m, where the coefficients are γ_m = 1/4, 1/3, 1/2 and 1, respectively. The residual $\tilde{\mathbf{R}}$ is defined as

$$\begin{aligned} \tilde{R} = &\frac{\partial \tilde{E}}{\partial \xi} + \frac{\partial \tilde{F}}{\partial \eta} + \frac{\partial \tilde{G}}{\partial \zeta} - \frac{\partial}{\partial \xi}\left(\frac{\tilde{D}}{J} g_{ij} \frac{\partial J\tilde{Q}}{\partial \xi}\right) - \frac{\partial}{\partial \eta}\left(\frac{\tilde{D}}{J} g_{ij} \frac{\partial J\tilde{Q}}{\partial \eta}\right) - \frac{\partial}{\partial \zeta}\left(\frac{\tilde{D}}{J} g_{ij} \frac{\partial J\tilde{Q}}{\partial \zeta}\right) - \tilde{S} \\ &- \frac{\varepsilon_2 \psi}{2J\Delta t}\left[\frac{\partial^2}{\partial \xi^2} + \frac{\partial^2}{\partial \eta^2} + \frac{\partial^2}{\partial \zeta^2}\right](J\tilde{Q}) - \frac{\varepsilon_4 \psi}{8J\Delta t}\left[\frac{\partial^4}{\partial \xi^4} + \frac{\partial^4}{\partial \eta^4} + \frac{\partial^4}{\partial \zeta^4}\right](J\tilde{Q}) \end{aligned} \tag{41}$$

A combination of second and fourth order artificial dissipation is necessary in EHD-type problems because of the existence of sharp gradients in the charged particle density distribution. The last two terms in equation (41) represent second and fourth order artificial dissipation (Steger and Kutler, 1977) terms which could be added to improve the stability of the scheme and to prevent (Lee, Dulikravich and Kosovic, 1991) the electric charge signs from changing locally in the flow field. The artificial dissipation sensor function, ψ, was based on a normalized value of the local gradient of the charge density distribution. The influence of artificial dissipation terms is controlled by ε_2 and ε_4 which are user-specified small parameters. To further enhance the convergence rate, implicit residual smoothing was used. Poisson's equation was discretized and numerically solved by ADI scheme for the smoothed residual after each stage of the Runge-Kutta iteration (Jameson, Schmidt and Turkel, 1981), that is,

$$(1 - \omega \delta_{\xi\xi})(1 - \omega \delta_{\eta\eta})(1 - \omega \delta_{\zeta\zeta}) \bar{R}_i = \tilde{R}^m{}_i \tag{42}$$

where the smoothing operator is denoted by δ and ω is a user-specified constant, $\bar{R}_i$ represents the smoothed residual, and $\delta_{\xi\xi}, \delta_{\eta\eta}, \delta_{\zeta\zeta}$ are the second derivatives evaluated using central differences.

4. BOUNDARY CONDITIONS

By introducing the artificial compressibility term in the continuity equation, the system of equations becomes hyperbolic. Therefore, boundary conditions have to be applied considering characteristic directions. Proper boundary conditions are determined from the nonconservative form of the transformed system (37)

$$\frac{\partial \tilde{Q}}{\partial t} + \tilde{A}\frac{\partial \tilde{Q}}{\partial \xi} + \tilde{B}\frac{\partial \tilde{Q}}{\partial \eta} + \tilde{C}\frac{\partial \tilde{Q}}{\partial \zeta} = \frac{\partial}{\partial \xi}\left(\frac{\tilde{D}}{J} g_{ij} \frac{\partial J\tilde{Q}}{\partial \xi}\right) + \frac{\partial}{\partial \eta}\left(\frac{\tilde{D}}{J} g_{ij} \frac{\partial J\tilde{Q}}{\partial \eta}\right) + \frac{\partial}{\partial \zeta}\left(\frac{\tilde{D}}{J} g_{ij} \frac{\partial J\tilde{Q}}{\partial \zeta}\right) + \tilde{S} \tag{43}$$

The eigenmatrix corresponding to the flux vector Jacobian $\tilde{A}$ is

$$\tilde{\Lambda} = \text{diag}(U\text{-}a, U\text{+}a, U, U, U, U) \tag{44}$$

where a is an equivalent local speed of sound

$$a = \sqrt{U^2 + \beta(\xi_{,x}^2 + \xi_{,y}^2 + \xi_{,z}^2)}. \tag{45}$$

It can be concluded that one of the eigenvalues is negative for the 'subsonic' case. Therefore, five variables must be specified as boundary conditions at the inlet and one variable corresponding to the negative eigenvalue at the exit.

Boundary conditions are imposed by premultiplying the boundary equations by the modal matrix **M** and thus transforming the system of equations into characteristic form. Furthermore, the equations are premultiplied by a selection matrix **L** to select the variable which will be computed from the equation. The equation corresponding to the point at the boundary is

$$\left[\mathbf{L}\mathbf{M}_{\xi}^{-1} + \frac{\partial \Omega}{\partial \tilde{Q}}\right]\Delta\tilde{Q} = -\gamma_m \Delta t \left[\mathbf{L}\mathbf{M}_{\xi}^{-1}\tilde{R}^{m-1} + \frac{\Omega^n}{\gamma_m \Delta t}\right] \tag{46}$$

The selection matrix and the boundary condition vector for the inlet boundary are

$$\mathbf{L} = \text{diag}(1,0,0,0,0,0) \tag{47}$$

$$\Omega = (0, u-u_p, v-v_p, w-w_p, \theta-\theta_p, q-q_p)^T \tag{48}$$

The selection matrix and the boundary condition vector for the exit boundary are

$$\mathbf{L} = \text{diag}(0,1,1,1,1,1) \tag{49}$$

$$\Omega = (p-p_p, 0,0,0,0,0)^T \tag{50}$$

Wall boundary conditions have the same form as the inlet boundary conditions, except for the pressure which is computed from the normal momentum equation (28) as

$$\mathbf{n} \cdot \nabla \bar{\bar{p}} = \mathbf{n} \cdot \left(\frac{1}{Re} \nabla \cdot (\eta' \nabla \mathbf{v}) + \frac{Gr\ \theta}{Re^2}\mathbf{g} + S_E\ q\ \mathbf{E}\right) \tag{51}$$

Boundary conditions for electric charges on the solid boundaries were of the Neumann type. The Poisson equation for the electric potential (Eq. 31) was solved separately during each global iteration using an ADI algorithm.

An extension of this formulation to include multiple charged species and an electrically non-neutral carrier fluid should be conceptually straightforward, although it would require a substantial increase in computational resources.

5. COMPUTATIONAL RESULTS

Based on the analytical formulation and the numerical algorithm, a two-dimensional EHD flow analysis computer code was written. All computations were performed remotely on the Cray-YMP computer at NASA Ames Research Center and postprocessed in our Computational Fluid Dynamics Laboratory at Penn State University.

5.1 Closed Container Electro-Thermo-Convection

We shall demonstrate an example of a fluid flow generated by the combination of an electric field and thermal buoyancy. The mechanism of such an instability can be seen by an analogy with the classical Benard problem. Electroconvective vortices (Eringen and Maugin, 1990a and 1990b; Lee, Dulikravich and Kosovic, 1991) analogous to thermoconvective vortices will be developed if sufficient electrical potential energy can be released by inverting a charged layer. We have chosen a closed rectangular container having AR = 3 and discretized it with a rectangular grid consisting of 60 x 30 grid cells that were symmetrically clustered towards the container walls. The container was filled with a homogeneously charged fluid. No artificial dissipation was used in this example and artificial compressibility parameter was $\beta = 10$. The non-dimensional parameters were chosen as $Gr = 900$, $Re = (Gr)^{1/2}$. $Ec = 1.28 \times 10^{-9}$, $Pr = 7.936$, $N_E = 5.042$, $Pr_E = 0.0143$, $S_E = 0.213$, $D_E = 1.11 \times 10^{9}$. In the first test case, we decided to simulate the thermo-electro-convective phenomena as if the container was full of an electrically conducting but neutral fluid. An external electric field was imposed by means of electrodes along the lower and the upper wall. A constant potential difference of 1400 Volts was maintained between the two electrodes and the distance between the electrodes was 1.67×10^{-3}m. A temperature difference of 22 K was maintained between the top and bottom walls, while the vertical walls were thermally insulated. Pressure at each of the four walls was computed using the normal momentum equation. Then, we assumed that the charged particles were uniformly injected through the lower wall while treating the top wall as an exit boundary for the charged particles since the side walls had a Neumann condition imposed on electric charges. Figure 1a depicts the resulting flow field consisting of two strong counterrotating vortices demonstrating the combined effects of the buoyancy driven flow and the electrically driven flow. In this case, Joule's heating and buoyancy force were taken into account and the isotherms are plotted in Figure 1b. Charge density contours are shown in Figure 1c confirming that the boundary conditions were satisfied accurately and indicating that charges stayed concentrated close to the bottom wall electrode which generated them. Figure 1d isopotential electric field lines, indicating the electric field distribution between the two electrodes. A closer look reveals that the electric currents generated by the flowfield are negligible compared to the externally applied electric field, thereby validating the assumption of neglecting magnetic induction effects.

A second test case was considered with a vertical closed rectangular container with an AR=0.33. The non-dimensional parameters for this case were $Gr=900$, $Re = (Gr)^{1/2}$. $Ec=1.28 \times 10^{-9}$, $Pr = 7.936$, $N_E = 2.521$, $Pr_E = 0.0071$, $S_E=0.426$, $D_E=1.11 \times 10^{9}$. The potential difference of 2800 V was maintained between the vertical walls, while the Neumann boundary condition was used for the electric field on the horizontal walls. As in the first test case a temperature difference of 22 K was maintained between the horizontal walls. Charges were injected from the left vertical wall and were absorbed by the right vertical wall. Figure 2a depicts the flowfield which consists of a single non-symmetric dominant vortex which conforms to the first convective mode observed at low Rayleigh numbers in closed vertical chambers (Muller, Neumann and Weber, 1984). The isotherms predicted in this case are shown in Figure 2b, illustrating a strong buoyancy driven flow. Strong charge density gradients near the left vertical electrode are illustrated in Figure 2c, while Figure 2d depicts the corresponding electric field.

5.2 Couette Flow With Electrically Charged Particles

It has been observed by a number of experimentalists that electrorheological fluids exibit increased viscosity when subjected to a progressively stronger electric potential field. This feature is exceptionally useful for a number of practical applications where it is desirable to actively control flow field dissipation of kinetic energy or heat transfer mode between conduction and convection. To demonstrate some aspects of such flows we have decided to compute two cases: one case with a uniform viscosity and another with a viscosity that directly depends on the local electric charge concentration. In both test cases a straight horizontal channel having AR = 10 and height of 0.1 m was descritized with 60 x 60 non-clustered grid cells. The main fluid was assumed to be electrically conductive but neutral. Electric charges were injected uniformly along the bottom stationary wall electrode, while the top wall electrode was moving to the right at a constant speed. Electric charges had an open boundary condition at the top moving wall and were assumed not to vary in the main stream direction at the flow inlet and flow outlet. A triangular velocity profile correspoding to a classical Couette flow was imposed at the inlet, while at the exit we used a characteristic boundary condition treatment for velocity. The artificial compressibility coefficient was $\beta = 1$ and Reynolds number was taken as $Re = 100$. This was based on $v_0 = 0.001$ m/s, $\rho_0 = 1000$ kg/m^3 and $\eta_o = 0.001$ kg/m/s. Fourth order dissipation was not used, while the coefficient of the second order dissipation introduced in the charge conservation equation only was $\varepsilon_2 = 0.0004$.

Non-dimensional parameters used in the first test case were $Gr = 0.Ec = 8.6 \times 10^{-9}$, $N_E = 3.53$, $Pr_E = 0.04$, $S_E = 4.16 \times 10^{-2}$, $D_E = 2.5 \times 10^{7}$. A uniform electric potential difference of 500 V was imposed between the top and the bottom walls. With the uniform viscosity, the computed velocity profile stayed for all practical purposes uniformly triangular throughout the channel (Fig. 3a). Electric charges that were injected at the bottom diffused only negligibly in the vertical direction (Fig. 3b) thus affecting somewhat the vertical distribution of the electric potential (Fig. 3c). The EHD system of equations in this test case converged very smoothly (Fig. 4).

In the second test case we used $Gr = 0.Ec = 8.6 \times 10^{-9}$, $N_E = 1.75$, $Pr_E = 0.02$, $S_E = 8.32 \times 10^{-2}$, $D_E = 2.5 \times 10^{7}$. A uniform electric potential difference of 1000 V was imposed between the top and the bottom walls. Pressure at the solid walls was calculated by the normal momentum equation, whereas at the exit non-reflecting boundary conditions (Dulikravich, Ahuja and Lee, 1993) were used. Here, the viscosity coefficient was modeled according to the formula $\eta = \eta_o 10^{C(q/q_0)}$ where the constant was taken as $C = 1$. In order to ensure stability of the computer code the variation of the local Reynolds number due to the variation in viscosity had to be taken into account in calculating the local time step at each node. This had an adverse effect on the convergence history (Fig. 4) but it ensured stability in the entire computational domain. The computed velocity profile in the case of variable viscosity deviates from the Couette triangular profile in the vicinity of the bottom wall (Fig. 5a) where the electrical charges are highly concentrated (Fig. 5b). Notice that in this case the charges (Fig. 5c) are far less concentrated near the bottom wall than those observed in the previous case with constant viscosity (Fig. 3c). The above phenomenon can be attributed to the stronger electric field imposed in this case coupled with reduction of the fluid speed near the bottom wall where the viscosity is very high.

6. CONCLUSIONS

An electrohydrodynamic flow model has been developed and computations including thermally and electrically induced motion have been performed using a finite difference method. The existence of electroconvective vortices analogous to thermoconvective vortices has been computationally demonstrated. In the case when local fluid viscosity is made dependent on the local concentration of electric charges it was found that the flow field velocity profiles were altered. Diffusion and convection of charged particles under the influence of a steady electric field has resulted in patterns that have been documented in literature. An extension of this work to a fully three-dimensional software package which will include a multi-species environment, dynamic currents large enough to include magnetic induction effects and time-dependent processes is deemed feasible.

7. ACKNOWLEDGMENTS

The authors express their gratitude to the NASA Lewis Research Center and to the NASA Ames Research Center NAS facility for the free use of their computers. Special thanks are due to Mr. Scott G. Sheffer and Mrs. Sheila Corl for their help in the final editing process of this paper. Graphics was performed on computing equipment donated by Apple Computer, Inc.

8. REFERENCES

1. Stuetzer, O. M., 1962, "Magnetohydrodynamics and Electrohydrodynamics," *The Physics of Fluids*, Vol. 5, No. 5, pp. 534-544.
2. Lee, S. and Dulikravich, G. S., 1991a, "Magnetohydrodynamic Steady Flow Computations in Three Dimensions", AIAA Paper 91-0388, Reno, NV; also in *International Journal for Numerical Methods in Fluids*, Vol.13, No. 7, pp. 917-936.
3. Dulikravich, G.S. and B. Kosovic, 1992, "Solidification of Variable Property Melts Under the Influence of Low Gravity, Magnetic Fields and Electric Fields," AIAA paper 92-0694, AIAA Aerospace Sciences Meeting, Reno, NV.
4. Dulikravich, G. S, Ahuja, V. and S. Lee, 1993, "Three-Dimensional Solidification With Magnetic Fields and Reduced Gravity," AIAA paper 93-0912, AIAA Aerospace Sciences Meeting, Reno, NV.
5. Landau, L. D. and Lifshitz, E. M., 1960, Electrodynamics of Continuous Media, Pergamon Press, New York.

6. Melcher, J. R., 1981, Continuum Electromechanics, The MIT Press, Cambridge, MA.
7. Babskii, V. G., Zhukov, M. Y. and Yudovich, V. I., 1989, "Mathematical Theory of Electrophoresis," (translated by C. Flick), Consultants Bureau, New York, N.Y.
8. Eringen, A. C., and Maugin, G. A., 1990a, Electrodynamics of Continua I; Foundations and Solid Media, Springer-Verlag, New York, N.Y.
9. Eringen, A. C., and Maugin, G. A., 1990b, Electrodynamics of Continua II; Fluids and Complex Media, Springer-Verlag, New York, N.Y.
10. Reitz, J. R., Fredrick, J. M., and Christy, R. W., 1979, Foundations of Electromagnetic Theory, Addison-Wesley Publishing Company.
11. Rhodes, H. P., Snyder, R. S. and Roberts, G. O., 1989, "Electrohydrodynamic Distortion of Sample Streams in Continuous Flow Electrophoresis," *Journal of Colloid and Interface Science*, Vol. 129, No. 1, pp. 78-90.
12. Changeart, J. F., Marsal, O., Sanchez, V., Zager, F., Costet, R. and Armadieu, P., 1986, "SELECTE: Scientific Instrument Devoted to Continuous Flow Electrophoretic Separation on Earth and in Space," *Proc. of 6th European Symposium of Material Sciences Under Microgravity Conditions*, Bordeaux, France, pp. 285-290; also ESA SP-256, Feb. 1987.
13. Bello, M. S. and Polezhaev, V. I., 1991, "Hydrodynamics, Gravitational Sensitivity and Transport Phenomena in Continuous Flow Electrophoresis," AIAA paper 91-0112, Aerospace Sciences Meeting, Reno, NV.
14. Lee, S., Dulikravich, G. S.and Kosovic, B., 1991, "Electrohydrodynamic (EHD) Flow Modelling and Computations", AIAA Paper 91-1469, AIAA Fluid, Plasma Dynamics and Lasers Conference, Honolulu, HI.
15. Gray, D. D., and Giorgini, A., 1976, "The Validity of the Bousinessq Approximation for Liquids and Gases," *International Journal of Heat and Mass Transfer*, Vol. 19, pp. 545-551.
16. Chorin, A. J., 1967, "A Numerical Method for Solving Incompressible Viscous Flow Problems," *Journal of Computational Physics*, Vol. 2, pp. 12-26.
17. Lee, S. and Dulikravich, G.S., 1991, "Performance Analysis of DMR Method for Acceleration of Iterative Algorithms," AIAA paper 91-0241, AIAA Aerospace Sciences Meeting, Reno, NV.
18. Jameson, A., Schmidt, W., and Turkel, E., 1981, "Numerical Solutions of the Euler Equations by Finite Volume Methods Using Runge-Kutta Time-Stepping Scheme," AIAA paper 81-1259, Palo Alto, CA.
19. Steger, J. L. and Kutler, P., 1977, "Implicit Finite-Difference Procedure for the Computation of Vortex Wakes," *AIAA Journal*, Vol. 15, No. 7, pp. 581-590.
20. Muller, G., Neumann, G. and Weber, W., 1984, "Natural Convection in Vertical Bridgman Configurations," *Journal of Crystal Growth*, Vol.70,pp. 78-93.

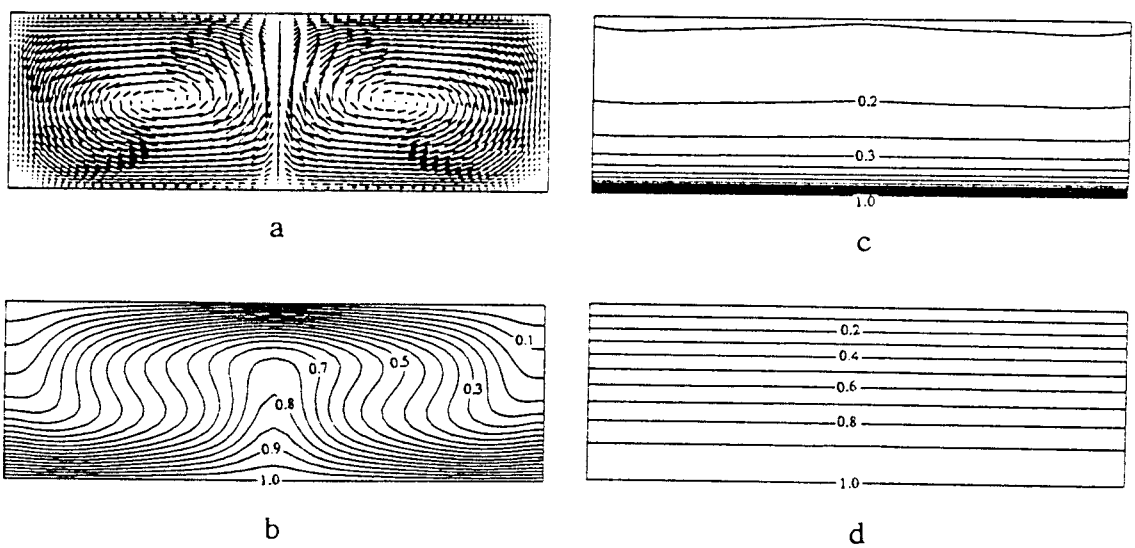

Fig. 1 Electro-thermo-convection in a horizontal closed container with hot bottom and cold top wall and an externally applied electric field of 1400 Volts between the horizontal walls: a) velocity field, b) isotherms, c) constant electric charge lines, and d) constant electric potential lines.

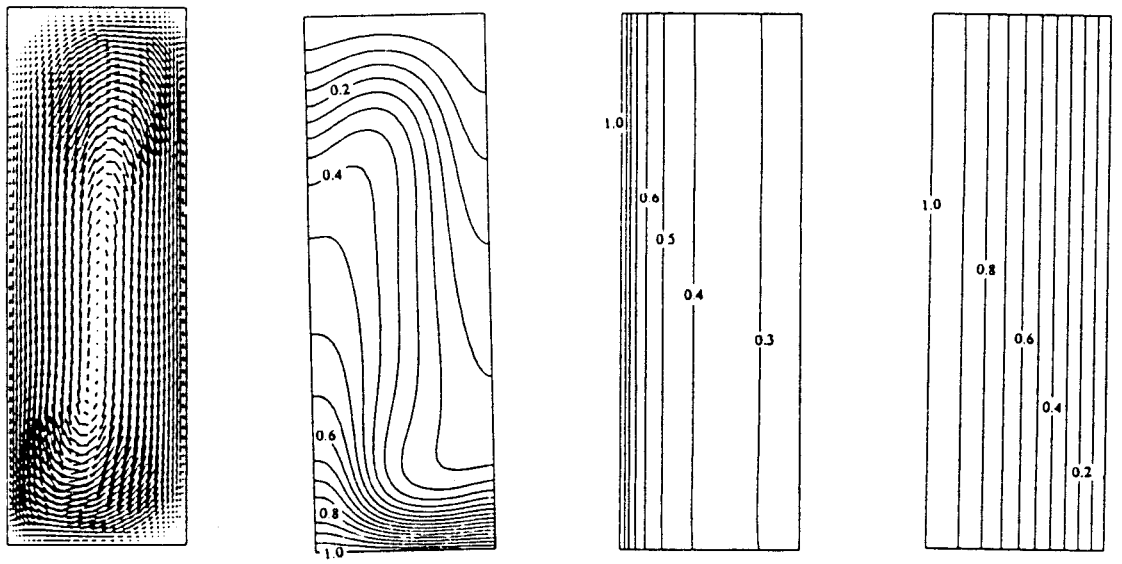

Fig. 2 Electro-thermo-convection in a vertical closed container with hot bottom and cold top walls and an externally applied electric field of 2800 Volts between the vertical walls: a) velocity field, b) isotherms, c) constant electric charge lines, and d) constant electric potential lines.

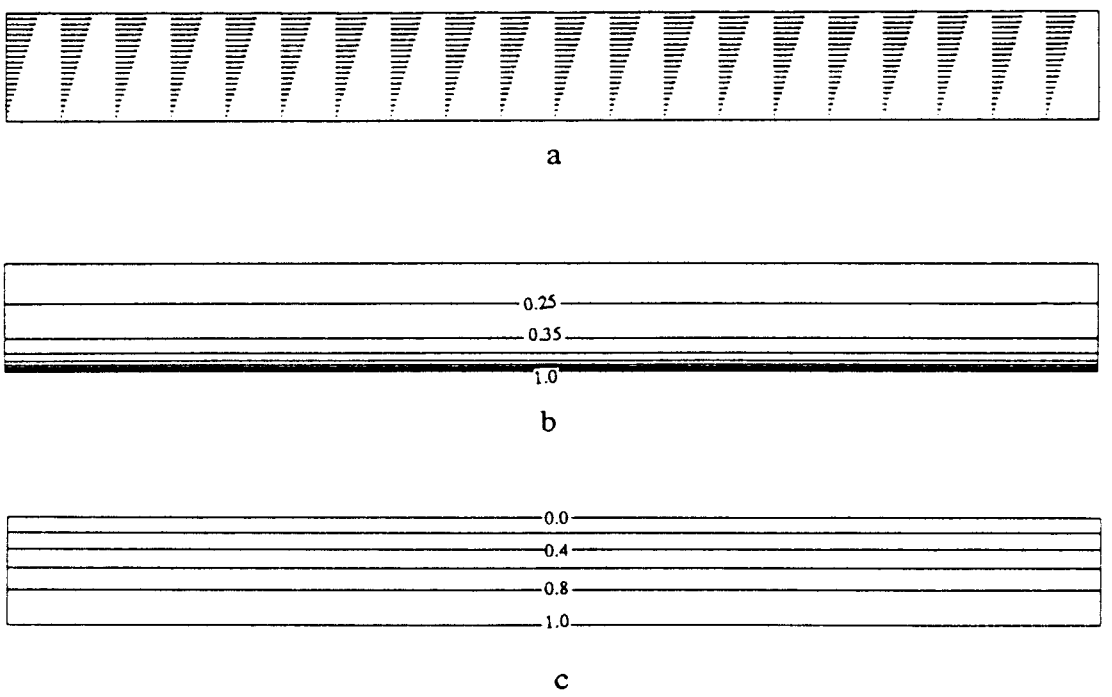

Fig. 3 Channel EHD-Couette flow with constant viscosity and 500 Volts between the walls: a) velocity profiles, b) constant electric charge lines, and c) constant electric potential lines.

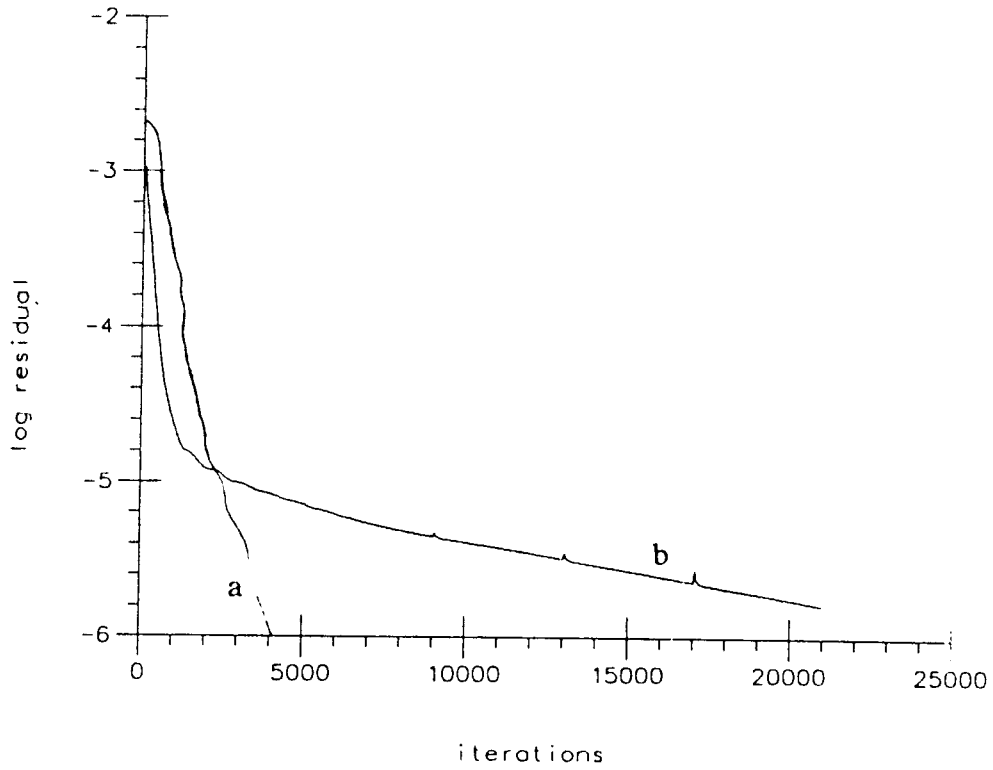

Fig. 4 Convergence histories for channel EHD-Couette flow: a) with constant viscosity and 500 Volts between the walls, b) with variable viscosity and 1000 Volts between the walls,.

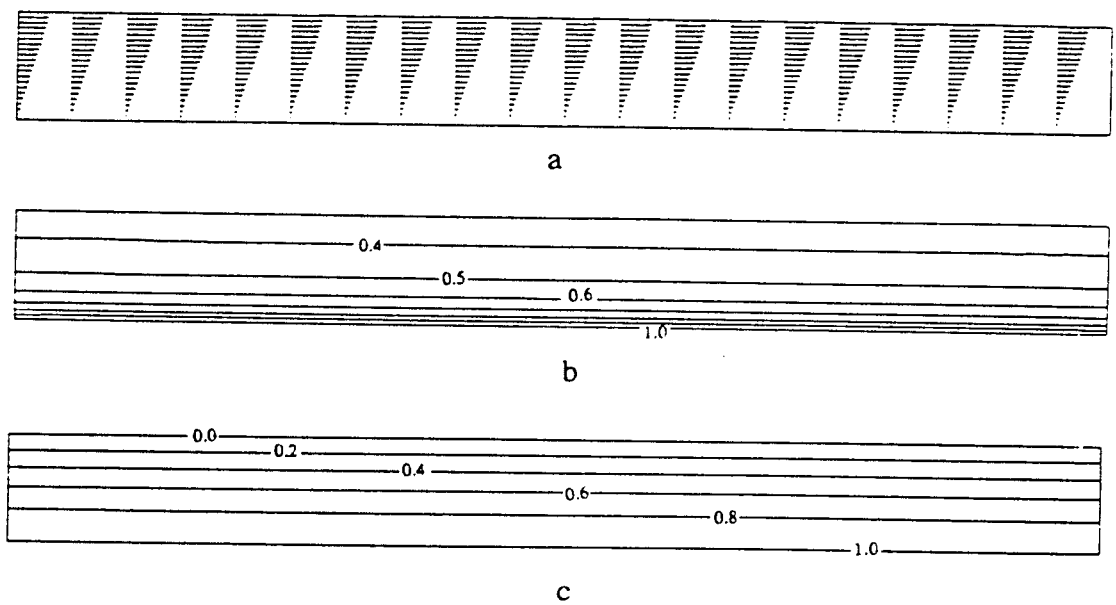

Fig. 5 Channel EHD-Couette flow with variable viscosity and 1000 Volts between the walls: a) velocity profiles, b) constant electric charge lines, and c) constant electric potential lines.